Electronic Supplementary Information

High Polarity Poly (vinylidene fluoride-*co*-trifluoroethylene) Random Copolymer with All-Trans Conformation for Solid-State $LiNi_{0.8}Co_{0.1}Mn_{0.1}O_2$/Lithium Metal Batteries

*Jian-Ping Zeng,[a] Jun-Feng Liu,[a] Hua-Dong Huang,[b] Shao-Cong Shi,[b] Ben-Hao Kang, [a] Chen Dai, [a] Liwei Zhang, [a] Zhichao Yan, [a] Florian J. Stadler,[a] Yan-Bing He,[c] Yan-Fei Huang[a,b]**

[a] *Shenzhen Key Laboratory of Polymer Science and Technology, Guangdong Research Center for Interfacial Engineering of Functional Materials, College of Materials Science and Engineering, Shenzhen University, Shenzhen 518055, P. R. China*

[b] *College of Polymer Science and Engineering, State Key Laboratory of Polymer Materials Engineering, Sichuan University, Chengdu 610065, P. R. China*

[c] *Shenzhen Geim Graphene Center, Institute of Materials Research, Tsinghua Shenzhen International Graduate School, Tsinghua University, Shenzhen, 518055, P. R. China*

Corresponding author: yanfeihuang@szu.edu.cn

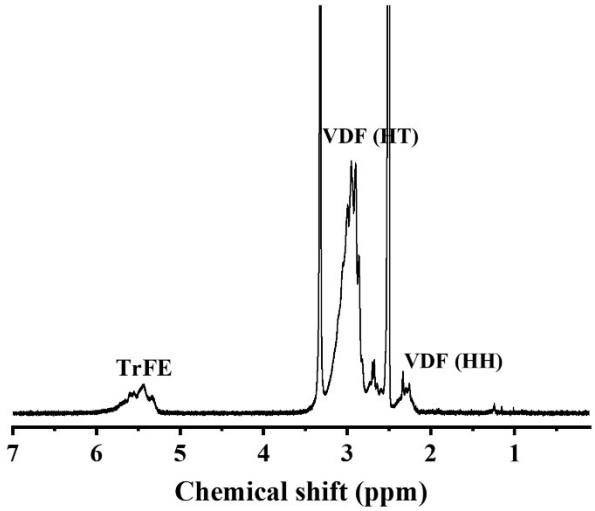

Fig. S1 The ^{1}H NMR spectra of the P(VDF-TrFE) 80/20 (mol./mol.) sample. DMSO-d_6 was used as the solvent.

As shown in Fig. S1, the peaks locate at ~5.6, 3.1, and 2.4 ppm are assigned to TrFE, -$CF_2CH_2CF_2CH_2CF_2$- sequence (VDF, head-to-tail, H-T), and -$CH_2CF_2CF_2CH_2$-sequence (VDF, head-to-tail, H-T), respectively. The sharp peaks at 2.5 and 3.3 ppm are assigned to DMSO-d_6 and water, respectively. The molar compositions are determined by the ^{19}F NMR results, as shown in Fig. S2 and Table S1.

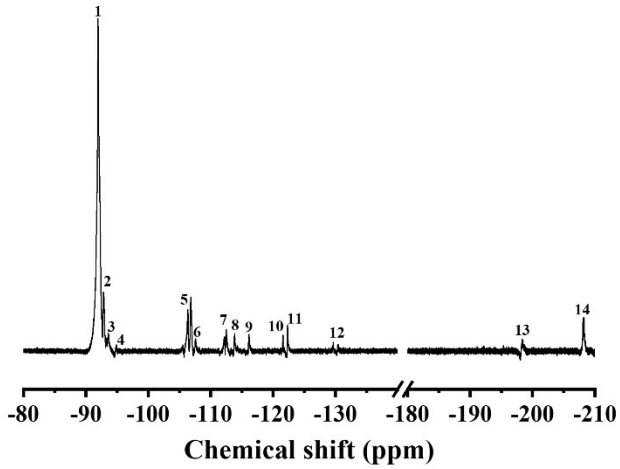

Fig. S2 The ^{19}F NMR spectra of the P(VDF-TrFE) 80/20 (mol./mol.) sample. DMSO-d_6 was used as the solvent. ^{19}F NMR peak assignments for the copolymer are listed in Table S1.

Table S1. ^{19}F NMR peak assignments for P(VDF-TrFE) 80/20 (mol./mol.) copolymer.

Peak No.	Sequence	Designation	Chemical Shift (ppm)
1	-$CF_2CH_2CF_2CH_2CF_2$-	VDF-VDF, H-T	-92.02
2	-$CF_2CH_2CF_2CH_2CF_2$-	VDF-VDF, H-T	-92.83
3	-$CHFCH_2CF_2CH_2CF_2$-	TrFE-VDF, T-T	-93.42
4	-$CHFCH_2CF_2CH_2CF_2$-	TrFE-VDF-VDF, T-T/H-T	-94.88
5	-$CF_2CHFCF_2CH_2CF_2$-	TrFE-VDF, H-T	-106.30 ~ -106.83
6	-$CH_2CH_2CF_2CHFCF_2$-	VDF-TrFE, H-T	-107.55
7	-$CF_2CH_2CF_2CF_2CHF$-	VDF-TrFE, T-T	-112.18 ~ -112.50
8	-$CF_2CH_2CF_2CF_2CHF$-	VDF-VDF-TrFE, H-T/H-H	-113.80
9	-$CH_2CF_2CF_2CH_2CH_2$-	VDF-VDF, T-T	-116.12
10	-$CF_2CHFCF_2CHFCF_2$-	TrFE-TrFE, H-T	-121.56
11	-$CHFCHFCF_2CF_2CHF$-	TrFE-TrFE, T-T	-122.34
12	-$CHFCHFCF_2CF_2CHF$	TrFE-TrFE-TrFE, T-T/H-H	-129.53 ~ -130.37
13	-$CF_2CF_2CHFCH_2CF_2$-	TrFE-VDF, T-T	-198.27
14	-$CH_2CF_2CHFCF_2CH_2$-	VDF-TrFE, H-T	-208.26

Peak assignments are referenced from Lu, Y. Y., et al. *Macromolecules* **2006,** *39*, 6962-6968.; Yang L., et al. *Macromolecules* **2014**, *47*, 8119-8125; Yang L., et al. *Nature* 2018, 562, 96-100.

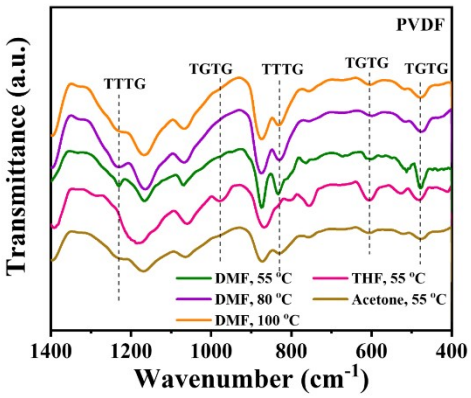

Fig. S3 The FTIR curves of PVDF films were prepared at different processing conditions. The peak positions and intensity change with varied processing methods, suggesting the conformation of PVDF changes at different processing conditions.

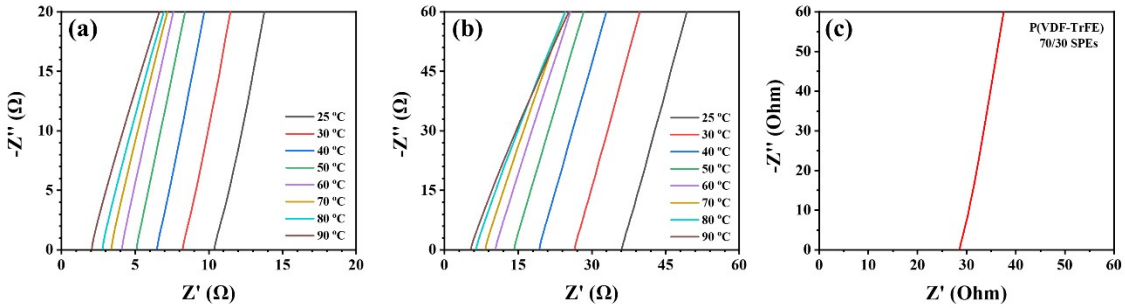

Fig. S4 EIS curves of (a) P(VDF-TrFE) SPEs and (b) PVDF SPEs sandwiched by two stainless plates of steel (SS) at varying temperatures. (c) EIS curve of P(VDF-TrFE) 70/30 mol% SPEs sandwiched by two stainless plates of steel (SS) at room temperatures.

Table S2. The electrochemical performance of LMBs employed different SPEs without any inorganic fillers.

SPEs	Ionic conductivity (S/cm)	Active material	Electrochemical performance	Ref.
P(VDF-TrFE) /LiTFSI	4.48×10^{-4} at 25 °C	NCM811	178, 161, and 145 mAh/g under 0.1, 1, and 2 C at 25 °C; 81.3% and 77.6% capacity retention after 600 cycles at 1C and 400 cycles at 2C	**This work**
PVDF/LiFSI	2.90×10^{-4} at 25 °C	NCM811	101 mAh/g after 60 cycles under 0.1 C at 25 °C	S1
P(VDF-TrFE-CTFE)/LiTFSI	3.10×10^{-4} at 25 °C	NCM811	149.1 mAh/g after 50 cycles under 0.1 C at 25 °C	S2
P(VDF-HFP) /LiTFSI	1.40×10^{-5} at 20 °C	$LiFePO_4$	70 mAh/g after 100 cycles under 0.5C at 25 °C	S3
P(VDF-HFP) /LiTFSI	$< 8.80 \times 10^{-5}$ at 25 °C	$LiFePO_4$	130 mAh/g after 100 cycles under 0.2 C at 55 °C	S4
PEO/LiTFSI	3.57×10^{-5} at 25 °C	$LiFePO_4$	130 mAh/g after 80 cycles under 0.1 C at 45 °C	S5
PEO/LiTFSI	5.40×10^{-5} at 30 °C	$LiFePO_4$	80 mAh/g after 100 cycles under 0.5 C at 60 °C	S6
PAN/$LiClO_4$	2.10×10^{-7} at 25 °C	——	——	S7
P(VDF-HFP) /LiTFSI	1.23×10^{-6} at 25 °C	——	——	S8

P(VDF-HFP) /$LiClO_4$	7.00×10^{-5} at 25 °C	——	——	S9
P(VDF-HFP) /$LiClO_4$	1.40×10^{-5} at 25 °C		——	S10
P(EGMA-co-HFBMA) /LiTFSI	1.45×10^{-4} at 70 °C	NCM523	120 mAh/g after 10 cycles under 0.1 C at 70 °C	S11
PVDF/LiTFSI	1.77×10^{-5} at 25 °C	$LiFePO_4$	22.4 mAh/g after 150 cycles under 0.5 C at 25 °C	S2

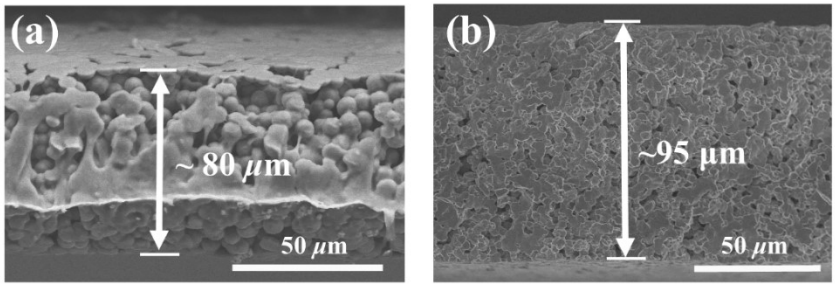

Fig. S5 The SEM images of the cross-section of (a) P(VDF-TrFE) SPEs and PVDF SPEs.

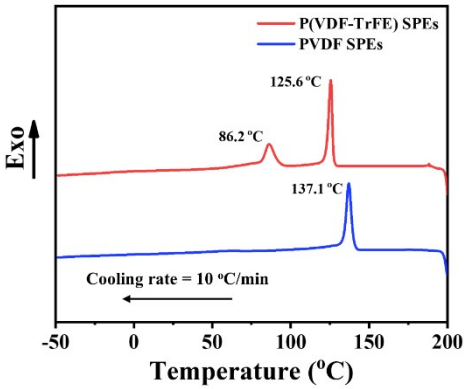

Fig. S6 DSC cooling curves of P(VDF-TrFE) SPEs and PVDF SPEs. The cooling rate is 10 °C/min.

As shown in Fig. S6, P(VDF-TrFE) SPEs have a smaller supercooling (i.e. the temperature gap between the crystallization temperature and film preparation temperature) than PVDF SPEs. This assures a more efficient time for crystallization, then resulting in a denser morphology of P(VDF-TrFE) SPEs than PVDF SPEs as shown in Figs. 3a and 3b.

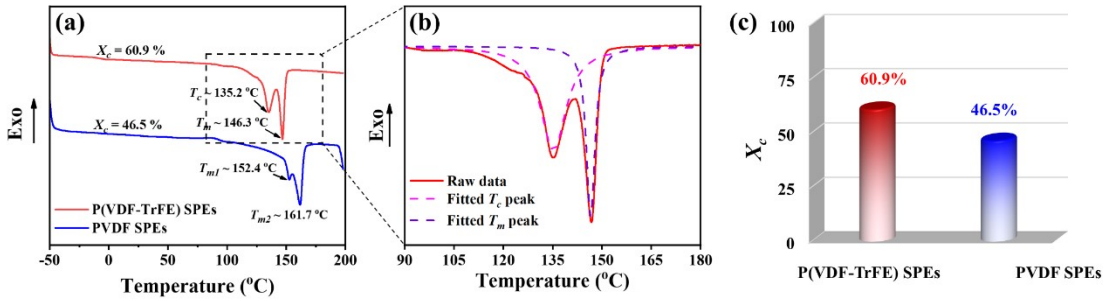

Fig. S7 (a) DSC 2nd heating curves of P(VDF-TrFE) SPEs and PVDF SPEs. (b) DSC fitting curves of P(VDF-TrFE) SPEs from (a) showing the T_c and T_m peaks. (c) The crystallinity of P(VDF-TrFE) SPEs and PVDF SPEs.

From the DSC heating curve (Fig. S7a), PVDF SPEs show two melting peaks 152.4 and 161.7 °C, respectively, which corresponds to the melting of lamellae with two different thicknesses. Crystallinity (X_c) was determined by integrating the enthalpy peak from 90 to 180 °C. Nothing that the heat of fusion for the perfect PVDF crystal is 104.6 J/g.[S12] As for P(VDF-TrFE) SPEs, two peaks at 135.2 and 146.3 °C correspond to the Curie transition temperature (T_c) and the melting point (T_m), respectively.[S13] Since the heat of fusion for perfect P(VDF-TrFE) 80/20 mol./mol. crystal has never been reported, here we use the value for perfect P(VDF-TrFE) 77/23 mol./mol. crystal, 38 J/g,[S14] to calculate the X_c of our P(VDF-TrFE) SPEs. Peak fitting was employed to differentiate the melting peak from the Curie transition peak as shown in Fig. S7b. X_c of P(VDF-TrFE) SPEs and PVDF SPEs are shown in Fig. S7c.

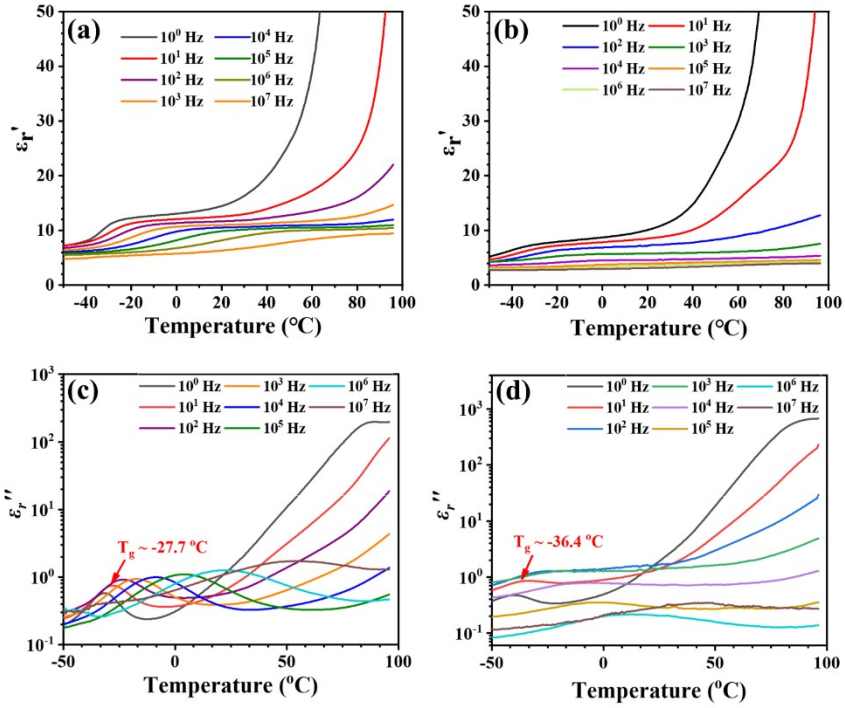

Fig. S8 (a, b) ε_r' and (c, d) ε_r'' as a function of temperature at varied frequencies for (a, c) P(VDF-TrFE) and (b, d) PVDF.

Table S3. T_g of P(VDF-TrFE) and PVDF obtained from Fig. S8c and 8d at varied frequencies.

Frequency	P(VDF-TrFE)	PVDF
10^0 Hz	-31.8 °C	-40.8 °C
10^1 Hz	-27.7 °C	-36.4 °C
10^2 Hz	-23.1 °C	-26.6 °C
10^3 Hz	-17.1 °C	-20.5 °C
10^4 Hz	-8.6 °C	-13.4 °C
10^5 Hz	-4.0 °C	-6.2 °C
10^6 Hz	22.1 °C	7.0 °C
10^7 Hz	53.8 °C	43.8 °C

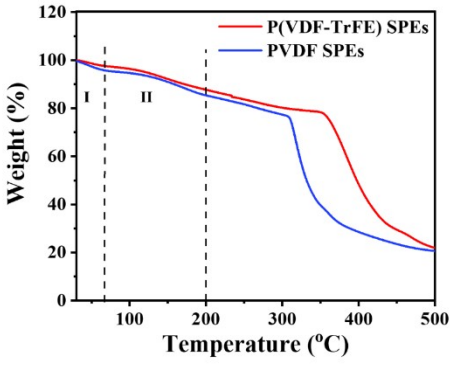

Fig. S9 TGA results of P(VDF-TrFE) SPEs and (b) PVDF SPEs.

The minor weight loss before 55 °C (region I) in Fig. S9 is due to the trapped moisture. The weight loss observed at 55-200 °C (region II) derives from the evaporation of residual DMF.[S2, S15] The residue of DMF is estimated to be only about 9.95 wt% and 10.32 wt% in P(VDF-TrFE) and PVDF SPEs, respectively.

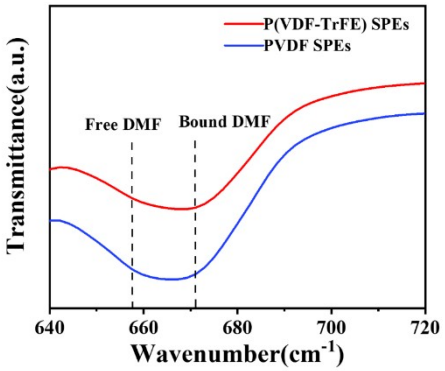

Fig. S10 FTIR spectra of DMF molecules in P(VDF-TrFE) SPEs and PVDF SPEs. The peak position for free and bound DMF locates at 658 and 673 cm^{-1}, respectively.[S2, S15, S16] The results show all residual DMF is in bonded form.

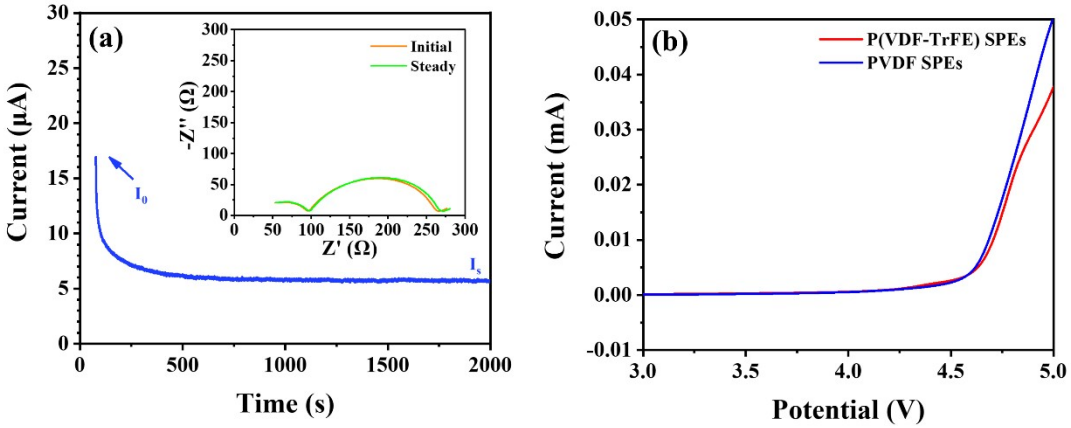

Fig. S11 (a) Chronoamperometry profiles of Li/PVDF SPEs/Li symmetrical cells under a polarization voltage of 10 mV. (b) LSV curves of P(VDF-TrFE) SPEs and PVDF SPEs at 25 °C.

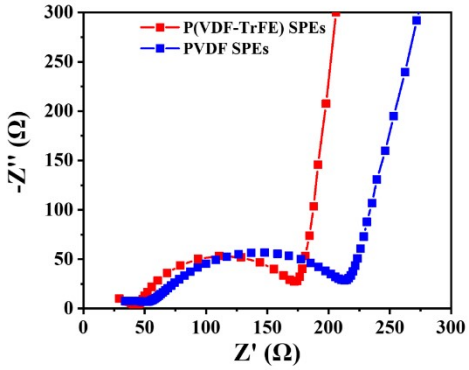

Fig. S12 EIS spectra of the NCM811/P(VDF-TrFE) SPEs/Li and NCM811/PVDF SPEs/Li cells at 25 °C.

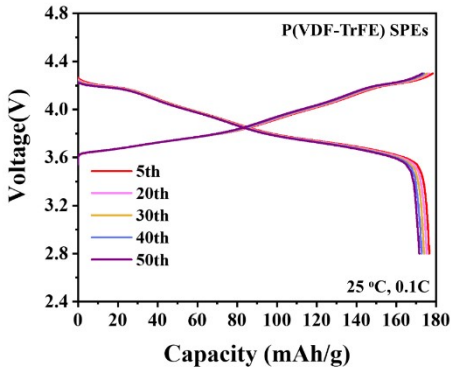

Fig. S13 Charge-discharge voltage profiles of NCM811/P(VDF-TrFE) SPEs/Li cells at varied cycles. The batteries were performed at 25 °C and 0.1 C.

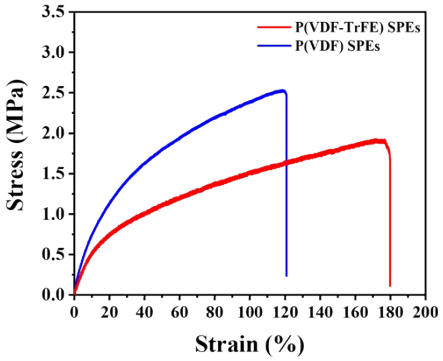

Fig. S14 Tensile properties of P(VDF-TrFE) and PVDF SPEs. The stretching rate is 10 mm/min.

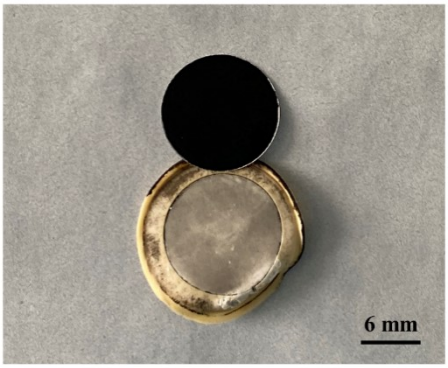

Fig. S15 The digital image of disassembled NCM811/PVDF SPEs/Li cell after 200 cycles at 1 C and 25 ºC showing a poor adhesion between PVDF SPEs and NCM811.

Reference

[S1] K. Yang, L. Chen, J. Ma, C. Lai, Y. Huang, J. Mi, J. Biao, D. Zhang, P. Shi, H. Xia, G. Zhong, F. Kang, Y. B. He, *Angew Chem. Int. Ed.* **2021**, 60, 24668.

[S2] Y.-F. Huang, T. Gu, G. Rui, P. Shi, W. Fu, L. Chen, X. Liu, J. Zeng, B. Kang, Z. Yan, F. J. Stadler, L. Zhu, F. Kang, Y.-B. He, *Energy Environ. Sci.* **2021**, 14, 6021.

[S3] Y. Li, W. Zhang, Q. Dou, K. W. Wong, K. M. Ng, *J. Mater. Chem. A* **2019**, 7, 3391.

[S4] J. Lu, Y. Liu, P. Yao, Z. Ding, Q. Tang, J. Wu, Z. Ye, K. Huang, X. Liu, *Chem. Eng. J.* **2019**, 367, 230.

[S5] Z. Wan, D. Lei, W. Yang, C. Liu, K. Shi, X. Hao, L. Shen, W. Lv, B. Li, Q.-H. Yang, F. Kang, Y.-B. He, *Adv. Funct. Mater.* **2019**, 29.

[S6] J. Wan, J. Xie, X. Kong, Z. Liu, K. Liu, F. Shi, A. Pei, H. Chen, W. Chen, J. Chen, X. Zhang, L. Zong, J. Wang, L. Q. Chen, J. Qin, Y. Cui, *Nat. Nanotechnol* **2019**, 14, 705.

[S7] W. Liu, N. Liu, J. Sun, P. C. Hsu, Y. Li, H. W. Lee, Y. Cui, *Nano Lett* **2015**, 15, 2740.

[S8] W. Zhang, J. Nie, F. Li, Z. L. Wang, C. Sun, *Nano Energy* **2018**, 45, 413.

[S9] X. Zhang, T. Liu, S. Zhang, X. Huang, B. Xu, Y. Lin, B. Xu, L. Li, C. W. Nan, Y. Shen, *J. Am. Chem. Soc.* **2017**, 139, 13779.

[S10] Y. Sun, X. Zhan, J. Hu, Y. Wang, S. Gao, Y. Shen, Y. T. Cheng, *ACS Appl. Mater. Interfaces* **2019**, 11, 12467.

[S11] M. Jia, P. Wen, Z. Wang, Y. Zhao, Y. Liu, J. Lin, M. Chen, X. Lin, *Adv. Funct. Mater.* **2021**, 31.

[S12] L. Yang, J. Ho, E. Allahyarov, R. Mu, L. Zhu, *ACS Appl. Mater. Interfaces* **2015**, 7, 19894.

[S13] R. Su, J.-K. Tseng, M.-S. Lu, M. Lin, Q. Fu, L. Zhu, *Polymer* **2012**, 53, 728.

[S14] N. Meng, X. Zhu, R. Mao, M. J. Reece, E. Bilotti, *J. Mater. Chem. C* **2017**, 5, 3296.

[S15] W. Liu, C. Yi, L. Li, S. Liu, Q. Gui, D. Ba, Y. Li, D. Peng, J. Liu, *Angew Chem. Int. Ed.* **2021**, 60, 12931.

[S16] X. Zhang, J. Han, X. Niu, C. Xin, C. Xue, S. Wang, Y. Shen, L. Zhang, L. Li, C.-W. Nan, *Batter. Supercaps.* **2020**, 3, 876.